Monthly Notices
of the
ROYAL ASTRONOMICAL SOCIETY

MNRAS **430,** 259–263 (2013) doi:10.1093/mnras/sts600

Integrated Sachs–Wolfe effect map recovery from NVSS and *WMAP* 7-yr data

R. B. Barreiro,[1]⋆ P. Vielva,[1] A. Marcos-Caballero[1,2] and E. Martínez-González[1]

[1]*Instituto de Física de Cantabria (CSIC-Univ. Cantabria), Avda. de Los Castros s/n, E-39005 Santander, Spain*
[2]*Departamento de Física Moderna (Univ. Cantabria), Avda. de Los Castros s/n, E-39005 Santander, Spain*

Accepted 2012 December 10. Received 2012 November 23; in original form 2012 August 11

ABSTRACT

We present a map of the cosmic microwave background (CMB) anisotropies induced by the late integrated Sachs–Wolfe effect. The map is constructed by combining the information of the *Wilkinson Microwave Anisotropy Probe* 7-yr CMB data and the NRAO VLA Sky Survey (NVSS) through a linear filter. This combination improves the quality of the map that would be obtained using information only from the large-scale structure data. In order to apply the filter, a given cosmological model needs to be assumed. In particular, we consider the standard Λ cold dark matter model. As a test of consistency, we show that the reconstructed map is in agreement with the assumed model, which is also favoured against a scenario where no correlation between the CMB and NVSS catalogue is considered.

Key words: methods: data analysis – methods: statistical – cosmology: observations – cosmic background radiation – large-scale structure of Universe.

1 INTRODUCTION

Recent observations, as cosmic microwave background (CMB), Type Ia supernovae or baryon acoustic oscillations (BAOs) agree in establishing a current accelerated expansion of the Universe (see Weinberg et al. 2012 for a recent review), which, despite some less popular interpretations, is believed to be caused by the presence of some dark energy (see Peebles & Ratra 2003 for a review). The nature of dark energy is one of the most puzzling issues in modern cosmology. The actual characteristics of this fluid are still unclear, although, up to date, good agreement is found between the observations and the predictions derived from the presence of a cosmological constant with an equation of state $p = -\rho$.

One of the classical probes of dark energy is given by a non-null contribution to the CMB anisotropies from the late integrated Sachs–Wolf effect (ISW; Sachs & Wolfe 1967), under the assumption of a spatially flat universe. The (linear) ISW fluctuations are higher at very large angular scales, but, in any case, much smaller than the primary CMB fluctuations. In a seminal work, Crittenden & Turok (1996) proposed the cross-correlation of the CMB fluctuations and the dark matter distribution (typically traced by galaxy catalogues) as a possible approach to detect the ISW. Soon after the release of the *Wilkinson Microwave Anisotropy Probe* (*WMAP*) data, Boughn & Crittenden (2004) reported the first detection of the ISW effect via the CMB and the galaxy number density field. Posterior works (e.g. Fosalba, Gaztañaga & Castander 2003; Pietrobon, Balbi & Marinucci 2006; Vielva, Martínez-González & Tucci 2006; Giannantonio et al. 2008; Ho et al. 2008; McEwen et al. 2008; Dupé et al. 2011; Schiavon et al. 2012) have confirmed the detection of the ISW effect by exploring several galaxy catalogues and cross-correlation techniques. Average detection is found at $\approx 3\sigma$.

Besides these works focused on the statistical detection of the ISW, more recently there have been attempts to recover the actual ISW fluctuations on the sky. In principle, an optimal ISW map could be derived from a 3D gravitational potential. This has been explored from very large simulations (e.g. Cai et al. 2010). The complexity to recover optimally the potential from surveys of galaxies with redshift information is challenging (e.g. Kitaura et al. 2009; Jasche et al. 2010), but very promising from the ISW studies point of view (e.g. Frommert, Enßlin & Kitaura 2008).

Other approaches can be followed from surveys where the redshift information is poor, or known only statistically. Barreiro et al. (2008) proposed to use jointly maps of CMB anisotropies and of the galaxy number density field to recover the ISW signal on the sky. Alternative works making use only of galaxy catalogue maps have been proposed afterwards: Granett, Neyrinck & Szapudi (2009) on LRGs from SDSS-DR6, or Francis & Peacock (2010) and Dupé et al. (2011) on 2MASS.

This paper presents an application of the approach described in Barreiro et al. (2008) to *WMAP* (Jarosik et al. 2011) and NVSS (Condon et al. 1998). The outline of the paper is as follows. The methodology is reviewed in Section 2. A description of the data used, as well as the fiducial theoretical model is presented in Section 3. In Section 4, we present the results. Finally, conclusions are given in Section 5.

⋆ E-mail: barreiro@ifca.unican.es

2 METHODOLOGY

In order to reconstruct the ISW map, we have used the linear covariance-based filter presented in Barreiro et al. (2008). We give here the outline of the method.

Since the filter is implemented in harmonic space, for simplicity, we will assume that the considered data sets are full-sky. Let us denote by $s_{\ell m}$ and $g_{\ell m}$ the harmonic coefficients of the ISW map and the large-scale structure (LSS) survey, respectively. The covariance matrix $\mathbf{C}(\ell)$ of the signals at each multipole ℓ is given by

$$\mathbf{C}(\ell) = \begin{pmatrix} C_\ell^g & C_\ell^{sg} \\ C_\ell^{sg} & C_\ell^s \end{pmatrix}, \tag{1}$$

where C_ℓ^g and C_ℓ^s correspond to the auto-spectra of the galaxies and ISW maps,[1] respectively, while C_ℓ^{sg} is the cross-power between both signals. To construct the filter, we will make use of the Cholesky decomposition of the covariance matrix, which satisfies $\mathbf{C}(\ell) = \mathbf{L}(\ell)\mathbf{L}^T(\ell)$, where $\mathbf{L}(\ell)$ is a lower triangular matrix. It can be trivially shown that the elements of the Cholesky matrix relate to the elements of $\mathbf{C}(\ell)$ as $L_{11} = \sqrt{C_\ell^g}$, $L_{12} = C_\ell^{sg}/\sqrt{C_\ell^g}$ and $L_{22} = \sqrt{|\mathbf{C}(\ell)|/C_\ell^g}$, where $|\mathbf{C}(\ell)|$ is the determinant of the covariance matrix at each ℓ mode.

The estimated ISW map $\hat{s}_{\ell m}$ at each harmonic mode is given by (see Barreiro et al. 2008 for details)

$$\hat{s}_{\ell m} = \frac{L_{12}(\ell)}{L_{11}(\ell)} g_{\ell m} + \frac{L_{22}^2(\ell)}{L_{22}^2(\ell) + C_\ell^n} \left(d_{\ell m} - \frac{L_{12}(\ell)}{L_{11}(\ell)} g_{\ell m} \right), \tag{2}$$

where $d_{\ell m}$ are the harmonic coefficients of the CMB map and C_ℓ^n is the power spectrum of the CMB signal without including the ISW. Therefore, to reconstruct the ISW map, we need to assume an underlying cosmological model that determines the auto- and cross-power spectra present in the previous equation.

It is interesting to note that the final reconstructed map has two contributions: the first term in the previous equation is given by a filtered version of the galaxies map while the second expression is a Wiener filter (WF; Wiener 1949) of a modified CMB data map. This modified data are simply constructed as the original CMB map minus the filtered survey. In the case that there is no correlation between the CMB and the LSS survey, the filter simply defaults to the WF of the CMB map: since there is no correlation between both signals, the galaxies map does not contribute to the final ISW reconstruction. If the information provided by the CMB map were not considered, the estimated ISW would be given just by the filtered galaxies map.

It can be easily shown that the expected value of the power spectrum of the estimated ISW is given by

$$\left\langle C_\ell^{\hat{s}} \right\rangle = \frac{(C_\ell^{sg})^2 \left(|\mathbf{C}(\ell)| + C_\ell^g C_\ell^n \right) + |\mathbf{C}(\ell)|^2}{C_\ell^g \left(|\mathbf{C}(\ell)| + C_\ell^g C_\ell^n \right)}. \tag{3}$$

It is well known that the power spectrum of the WF reconstruction is biased towards values lower than the true signal, with the bias depending on the signal-to-noise ratio of the data. Since our signal is partially reconstructed using this filter, it will also be biased. The larger the cross-correlation between CMB and the considered galaxies catalogue, the smaller the bias, since the WF part will contribute relatively less than the filtered survey term (see Barreiro et al. 2008 for details).

[1] Note that C_ℓ^g corresponds to the power spectrum of the observed galaxies map and thus, in a general case, it will contain a noise contribution, while C_ℓ^s refers to the power spectrum of an ideal ISW map.

It is also straightforward to show that the expected cross-correlation between the recovered signal and the galaxies catalogue is equal to that of the assumed model. However, this is only correct if the assumed cross- and auto-power spectra reflect the underlying statistical properties between the ISW and the LSS survey. For instance, if we assume a non-vanishing cross-correlation in our model, while the data have zero correlation, our reconstructed ISW map would actually present a non-zero correlation with the LSS survey. However, this spurious correlation, whose expected value can be easily derived from equation (2), would be different from the one assumed in our model. In practice, the difference between the expected values of the cross-correlation for two (reasonably) different models will in general be small and, given the weakness of the signal and the statistical uncertainties, it may be difficult to discriminate between them. In any case, as we will see in Section 4, the comparison between the expected and estimated values of the cross-correlation is an interesting consistency check.

The previous description assumes that full-sky data are available. However, in practice, a mask will be needed to exclude those regions, in both CMB and galaxies survey maps, that have not been observed or are too contaminated to be included in the analysis. In Barreiro et al. (2008), it was shown that the method was robust against the presence of a mask and that the quality of the reconstruction was not significantly affected. Therefore, to deal with this problem, we will simply substitute in the previous equations the harmonic coefficients and power spectra by those obtained after masking the data with the considered mask. In particular, the *masked* version of the fiducial model for the power spectra will be obtained in the manner of MASTER (Hivon et al. 2002). In addition, we will make use of an apodized version of the considered mask in order to reduce the correlations between harmonic modes that are introduced on an incomplete sky.

3 DATA DESCRIPTION

In order to reconstruct the ISW map using the previous methodology, we need both a CMB map and an LSS catalogue, as well as a cosmological fiducial model. For the latter, we have assumed a Λ cold dark matter (ΛCDM) model that best fits *WMAP* 7-yr data, BAO and H_0 measurements (Komatsu et al. 2011).

For the CMB, we have made use of the *WMAP* 7-yr data (Jarosik et al. 2011) publicly available at the Legacy Archive for Microwave Background Data Analysis.[2] In particular, we have constructed a CMB map as a noise-weighted combination of the foreground reduced *V*- and *W*-band maps. The map has then been downgraded to a HEALPIX resolution of $N_{\rm side} = 32$. To reduce the galactic foreground contamination, the KQ85 mask provided by the *WMAP* team has been used. However, since we have to downgrade the mask to a lower resolution, we have not included in the mask the holes due to point sources since their contribution is expected to be negligible at the considered scales. The *WMAP* data, with the considered mask applied, are given in the top panel of Fig. 1.

Regarding the LSS catalogue, we have used the NRAO VLA Sky Survey (NVSS; Condon et al. 1998). NVSS covers the north hemisphere of the sky and part of the south until $\delta = -40^\circ$. The NVSS catalogue has nearly 2×10^6 discrete sources with fluxes above 2.5 mJy. The catalogue was made using two different configurations (D and DnC) of the Very Large Array (VLA). This introduced a declination dependence in the number of sources, specially for the

[2] http://lambda.gsfc.nasa.gov/

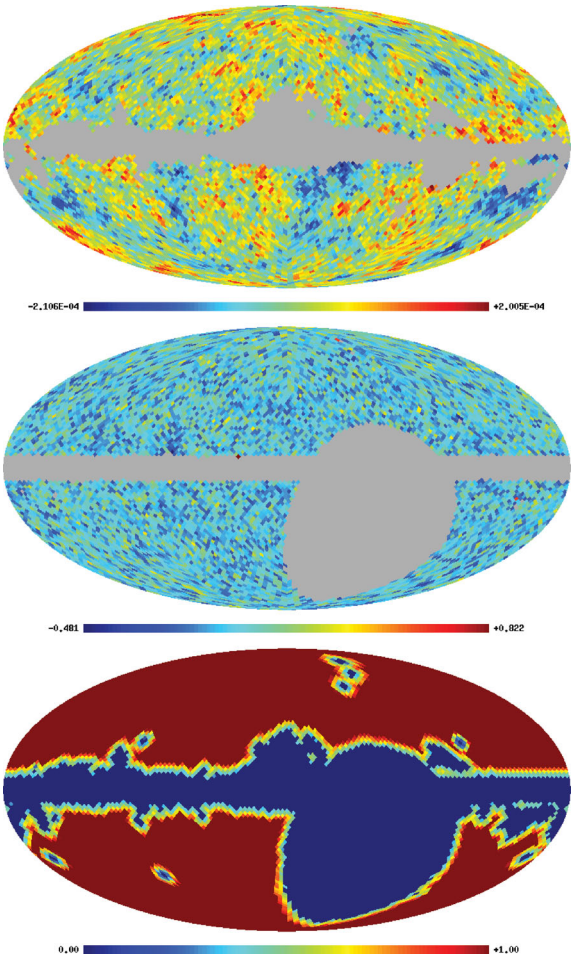

Figure 1. Top: *WMAP* 7-yr data (in Kelvin thermodynamic temperature). Middle: NVSS galaxy density number field. Bottom: apodized mask used for the analysis.

faintest ones. Sources above 5.0 mJy have been selected to build a catalogue not affected by this declination effect. The NVSS mask is defined by the unobserved sky, plus the sources within 7° from the galactic plane, as well as some regions associated with very near objects. The complete mask associated with NVSS leaves 73 per cent of the sky. The map is shown in the middle panel of Fig. 1.

The ISW-NVSS angular cross-power spectrum is calculated using the galaxy redshift distribution proposed by de Zotti et al. (2010): a polynomial fit to the CENSORS data (Brookes et al. 2008). For the galaxy bias, a redshift dependence as the one proposed by Xia et al. (2011) is assumed, where the bias is just defined by the minimum halo mass associated with NVSS radio-galaxies. The value of this mass is determined by fitting the NVSS angular power spectrum (see Marcos-Caballero et al., in preparation).

As it is well known (e.g. Hernández-Monteagudo 2010), there is a clear discrepancy between the measured NVSS auto-power spectrum and the theoretical model as described above. In particular, an excess of power at low multipoles is observed. This deviation does not seem to be related to the declination effect previously mentioned, since it is observed even for the angular power spectrum estimated from very bright sources. A possible explanation in terms of a non-linear evolution of the galaxy bias (caused by a primordial non-Gaussianity of the primordial perturbations) has been considered by Xia et al. (2011), although it would imply a value of the non-linear coupling parameter $f_{\rm NL}$ larger than the one obtained from other observables (as the CMB bi-spectrum estimated from *WMAP*; see, for instance, Curto, Martínez-González & Barreiro 2012). Currently, the nature of this discrepancy is not clear. Since the filter described in the previous section (see equation 2) is very sensitive to the value of the auto-power spectrum of the galaxy survey, we have used for C_ℓ^g a smooth fit to the observed NVSS spectrum (plus a Poissonian term contribution) instead of the theoretical model.

Finally, we have combined the *WMAP* and NVSS masks, leaving a useful area of 66 per cent. The mask is then apodized with a cosine function (using 3 pixels, i.e. $\sim 5^\circ.5$, for the size of the transition region with values between 0 and 1), in order to reduce the correlations among the harmonic modes of the incomplete sky. This apodized mask (see bottom panel of Fig. 1) is applied to the CMB and NVSS data prior to the reconstruction of the ISW map. In addition, the monopole and dipole outside the combined mask are subtracted prior to the construction of the ISW map.

4 ISW RECONSTRUCTION

Following the described methodology, we have produced an ISW map from the *WMAP* and NVSS data. The map is given in Fig. 2 and has been constructed at a HEALPIX resolution of $N_{\rm side} = 32$ and up to a maximum multipole $l = 95$.

As a consistency test, we have obtained the cross-correlation between the reconstructed ISW map and the NVSS data and compared it with the fiducial model. The former has been simply obtained as the pseudo-cross-spectrum from the masked maps, then corrected in the manner of MASTER and finally binned. In addition, we have also repeated the same procedure on two sets of 10 000 simulations. For the first set, we have constructed correlated CMB and NVSS-like simulations (generated as explained in Barreiro et al. 2008), assuming the same power spectra as for reconstructing the ISW map. For the second set, the auto-spectra are the same but zero correlation is assumed between the CMB and NVSS simulations. In both cases, we have included the corresponding Poissonian noise in the simulations of the galaxies catalogue. The results for this test are given in Fig. 3.

As expected, the average value (red triangles) for the correlated simulations agrees well with the considered model (black line). More interestingly, the data (blue asterisks) are also compatible with these simulations; this provides a good consistency check for our procedure and indicates that the assumed cross- and auto-spectra are reasonably close to the true statistical properties of the sky.

Conversely, the average obtained from the uncorrelated simulations (green squares) is biased with respect to the assumed cross-spectrum. This is expected, since the assumed model is not the same as the underlying true power spectrum. In particular, if we assume a model with positive correlation for simulated data which actually have zero correlation, the recovered ISW map would present a spurious correlation with the NVSS data. More specifically, from equation (2), it is easy to show that this spurious correlation is, on average, lower than the one assumed for the model. Therefore, this could serve as a consistency test to check if the considered model describes well the data. Unfortunately, since the signal is very weak, the difference between both cases is also small and it is difficult to distinguish between both hypotheses with this test.

To try to quantify which hypothesis is favoured by the data, we have calculated the goodness-of-fit difference:

$$\Delta\chi^2 = \chi_c^2 - \chi_u^2,$$

where

$$\chi_i^2 = \boldsymbol{c}_{\rm sg}\mathbf{M}_i^{-1}\boldsymbol{c}_{\rm sg}{}^{\rm T}, \quad (4)$$

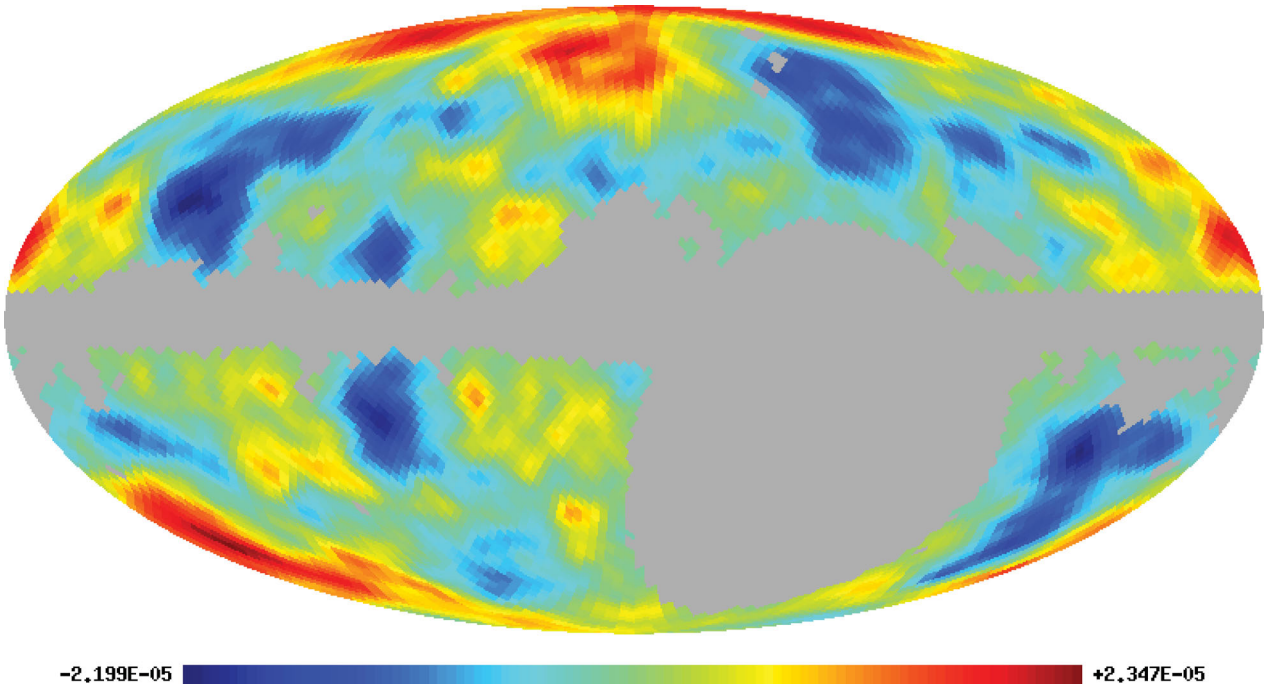

Figure 2. Reconstructed ISW map. Units are Kelvin (thermodynamic temperature).

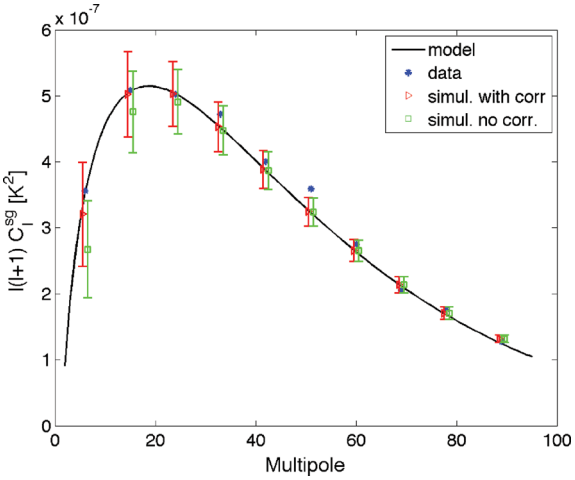

Figure 3. The binned cross-correlation between the reconstructed ISW map and the NVSS data is given (blue asterisks). For comparison, the fiducial model (black line) and the average and dispersion from two sets of 10 000 simulations are also shown. The red triangles and their error bars correspond to CMB and NVSS-like simulations which are correlated, while for the second set of simulations (green squares represent error bars), no correlation is introduced. The width of the bins is $\Delta_\ell = 9$, except for the last bin that is $\Delta_\ell = 13$. For a better visualization, the results for the simulations have been shifted with respect to the central value of the bin.

$i \equiv \{\mathrm{c}, \mathrm{u}\}$, and $\boldsymbol{c}_{\mathrm{sg}}$ corresponds to the vector constructed with the values of the binned cross power spectrum (the binning scheme is the same as that of Fig. 3). $\mathbf{M}_{\mathrm{c}}$ is the covariance matrix of the cross-spectrum obtained from 10 000 correlated simulations and $\mathbf{M}_{\mathrm{u}}$ the same matrix for the uncorrelated simulations set. We have calculated the distribution of this quantity from independent sets of 10 000 correlated and uncorrelated simulations and compare it to the value found for the data. In particular, we find $\Delta\chi^2(\mathrm{data}) = -2.4$. For the correlated CMB and galaxies survey simulations, we find that 28.9 per cent of the simulations have a value larger than the one obtained for the data. This percentage is reduced to 6.7 per cent, when we compare the data with the distribution obtained for uncorrelated simulations. Therefore, although the data are in fact compatible with the two cases considered, they favour the hypothesis of having an underlying correlation. This further confirms the consistency of our results.

Although, given the weakness of the considered cross-correlation, the power of these tests is somewhat limited, the fact that the data show consistency with the assumed model should not be taken for granted, since other assumptions may also affect the results. For instance, if we use the theoretical model to construct the auto-spectrum of the NVSS map, instead of a smooth fit to the measured data (as explained in Section 3), we find a clear departure of the cross-correlation between the reconstructed ISW map and the NVSS data with respect to the expected value.

Using simulations, we have also studied what is the improvement from combining both the CMB and NVSS data, with respect to using only the galaxies catalogue (as for instance in Dupé et al. 2011 whose proposed reconstruction corresponds to the term given by the filtered survey of equation 2). In particular, we find an improvement of 15 per cent in the error of the ISW reconstruction when the CMB data are included. In any case, the relative contribution to the reconstruction of the CMB and LSS data depends significantly on the cross-correlation between them, so it will differ for other galaxies surveys.

In a related matter, we can also calculate the expected relative contribution of the auto- and cross-power of the CMB and the galaxy number density maps to the angular power spectrum of the reconstructed ISW map (using equation 2). This is shown in Fig. 4 for the fiducial model as well as the actual contribution of each angular power spectrum for the considered data. As can be seen, the contribution from the power spectrum of the CMB C_ℓ^t is dominant at low multipoles (up to $\ell \approx 10$), while C_ℓ^g gives the main weight at

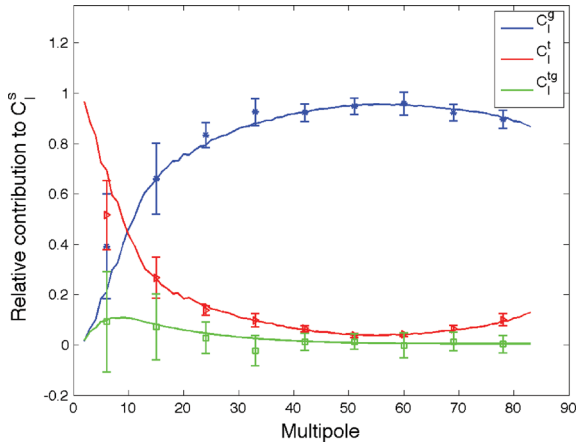

Figure 4. The expected relative contribution of the CMB and NVSS auto- and cross-spectra to the power spectrum of the ISW reconstruction is shown (solid lines) as well as the same quantities for the data. The results for the data have been binned to allow for a clearer comparison. The error bars correspond to the dispersion of the values within the considered bin.

higher multipoles. The contribution from the cross-power between the CMB and NVSS is subdominant at all multipoles. The results obtained from the data agree quite well with the expected value. However, it is interesting to point out that the relative importance of C_ℓ^t with respect to C_ℓ^g for the data is lower than the expectation value. This can be easily explained by the fact that the amplitude of the low multipoles of the *WMAP* data is lower than that of the fiducial model.

5 CONCLUSIONS

We have presented a reconstructed map of the ISW effect, obtained by combining through a linear filter CMB and LSS data. In particular, we have used the *WMAP* 7-yr data and the NVSS galaxies catalogue. The joint combination of both data sets improves by a 15 per cent the error of the ISW reconstruction in comparison to the case when only the NVSS data are used. We have performed a consistency test, showing good agreement between the cross-correlation inferred from the reconstructed ISW map and the assumed fiducial model. In particular, the data favour a ΛCDM model with respect to a scenario with null correlation between the CMB and the NVSS data. The relative contribution to the angular power spectrum of the ISW reconstructed map is dominated by the CMB fluctuations up to $\ell \approx 10$ and by the density number galaxies field at larger multipoles.

The presented methodology works in harmonic space, which implies the use of surveys with large sky coverage, in order to avoid the problematics introduced by large masks. However, this technique can be easily extended to work directly in the pixel space, which would make straightforward to deal with a mask and, in particular, LSS surveys with smaller sky coverage could also be used to reconstruct the ISW signal (Bonavera et al., in preparation). In addition, several catalogues can be combined at the same time, provided the covariance matrix between the surveys and the CMB data is known.

Finally, let us remark that the application of the approach described in this paper to future surveys [as EUCLID (Refregier et al. 2010) or J-PAS (Benítez et al. 2009), with very large sky coverage and very accurate redshift estimation] could provide maps of the ISW anisotropies caused by the LSS at different redshift shells. This will provide a tomographic view of the ISW fluctuations.

ACKNOWLEDGMENTS

We thank Andrés Curto, Raúl Fernández-Cobos and Francesco Paci for useful discussions. We acknowledge partial financial support from the Spanish Ministerio de Economía y Competitividad AYA2010-21766-C03-01 and Consolider-Ingenio 2010 CSD2010-00064 projects. PV also acknowledges financial support from the Ramón y Cajal programme and AMC thanks the Spanish Ministerio de Economía y Competitividad for a pre-doctoral fellowship. We also acknowledge the use of Legacy Archive for Microwave Background Data Analysis (LAMBDA). Support for it is provided by the NASA Office of Space Science. The HEALPIX package (Górski et al. 2005) was used throughout the data analysis.

REFERENCES

Barreiro R. B., Vielva P., Hernandez-Monteagudo C., Martinez-Gonzalez E., 2008, IEEE J. Sel. Top. Signal Process., 2, 747
Benítez N. et al., 2009, ApJ, 691, 241
Boughn S., Crittenden R., 2004, Nat, 427, 45
Brookes M. H., Best P. N., Peacock J. A., Röttgering H. J. A., Dunlop J. S., 2008, MNRAS, 385, 1297
Cai Y.-C., Cole S., Jenkins A., Frenk C. S., 2010, MNRAS, 407, 201
Condon J. J., Cotton W. D., Greisen E. W., Yin Q. F., Perley R. A., Taylor G. B., Broderick J. J., 1998, AJ, 115, 1693
Crittenden R. G., Turok N., 1996, Phys. Rev. Lett., 76, 575
Curto A., Martínez-González E., Barreiro R. B., 2012, MNRAS, 426, 1361
de Zotti G., Massardi M., Negrello M., Wall J., 2010, A&AR, 18, 1
Dupé F.-X., Rassat A., Starck J.-L., Fadili M. J., 2011, A&A, 534, A51
Fosalba P., Gaztañaga E., Castander F. J., 2003, ApJ, 597, L89
Francis C. L., Peacock J. A., 2010, MNRAS, 406, 14
Frommert M., Enßlin T. A., Kitaura F. S., 2008, MNRAS, 391, 1315
Giannantonio T., Scranton R., Crittenden R. G., Nichol R. C., Boughn S. P., Myers A. D., Richards G. T., 2008, Phys. Rev. D, 77, 123520
Górski K. M., Hivon E., Banday A. J., Wandelt B. D., Hansen F. K., Reinecke M., Bartelmann M., 2005, ApJ, 622, 759
Granett B. R., Neyrinck M. C., Szapudi I., 2009, ApJ, 701, 414
Hernández-Monteagudo C., 2010, A&A, 520, A101
Hivon E., Górski K. M., Netterfield C. B., Crill B. P., Prunet S., Hansen F., 2002, ApJ, 567, 2
Ho S., Hirata C., Padmanabhan N., Seljak U., Bahcall N., 2008, Phys. Rev. D, 78, 043519
Jarosik N. et al., 2011, ApJS, 192, 14
Jasche J., Kitaura F. S., Li C., Enßlin T. A., 2010, MNRAS, 409, 355
Kitaura F. S., Jasche J., Li C., Enßlin T. A., Metcalf R. B., Wandelt B. D., Lemson G., White S. D. M., 2009, MNRAS, 400, 183
Komatsu E. et al., 2011, ApJS, 192, 18
McEwen J. D., Wiaux Y., Hobson M. P., Vandergheynst P., Lasenby A. N., 2008, MNRAS, 384, 1289
Peebles P. J., Ratra B., 2003, Rev. Mod. Phys., 75, 559
Pietrobon D., Balbi A., Marinucci D., 2006, Phys. Rev. D, 74, 043524
Refregier A., Amara A., Kitching T. D., Rassat A., Scaramella R., Weller J., Euclid Imaging Consortium f. t., 2010, arXiv:e-prints
Sachs R. K., Wolfe A. M., 1967, ApJ, 147, 73
Schiavon F., Finelli F., Gruppuso A., Marcos-Caballero A., Vielva P., Crittenden R. G., Barreiro R. B., Martinez-Gonzalez E., 2012, MNRAS, 427, 3044
Vielva P., Martínez-González E., Tucci M., 2006, MNRAS, 365, 891
Weinberg D. H., Mortonson M. J., Eisenstein D. J., Hirata C., Riess A. G., Rozo E., 2012, arXiv:e-prints
Wiener N., 1949, Extrapolation, Interpolation and Smoothing of Stationary Time Series. Wiley, New York
Xia J.-Q., Baccigalupi C., Matarrese S., Verde L., Viel M., 2011, J. Cosmology Astropart. Phys., 8, 33

This paper has been typeset from a TEX/LATEX file prepared by the author.